

Nucleosynthesis in evolved stars with the NACRE* compilation

A. Palacios¹, F. Leroy²,
C. Charbonnel¹ and M. Forestini²

¹ Laboratoire d'Astrophysique de Toulouse, CNRS UMR 5572, France

² Laboratoire d'Astrophysique de l'Observatoire de Grenoble, CNRS UMR 5571, France

Abstract: Nucleosynthesis in evolved (RGB and AGB) low-mass stars is reviewed under the light of the reaction rates recommended in the NACRE compilation (Angulo et al. 1999). We use a parametric model of stellar nucleosynthesis to investigate the uncertainties that still exist nowadays on the nuclear data and to give a critical point of view on the resulting evolution of the chemical abundances. We discuss in particular (i) the NeNa and MgAl modes of hydrogen burning in the context of the chemical anomalies observed in RGB globular cluster stars, (ii) the helium combustion in a thermal pulse of an AGB star.

1 Nucleosynthesis and abundance anomalies in RGB stars

Proton capture nucleosynthesis inside the CNO, NeNa and MgAl loops, is advocated to account for abundances anomalies observed at the surface of GCRGs (Globular Cluster Red Giants), either in the context of the primordial scenario or evolutionary scenario (see Sneden and Charbonnel et al. in this volume). We focus here on the evolutionary scenario in order to determine to what extent it can account for the observations from a nuclear point of view. We present results for a $0.83M_{\odot}$, $[\text{Fe}/\text{H}] = -1.5$ model which is typical of a RGB star in the globular cluster M13.

For our calculations we use the nuclear reaction rates recommended by the NACRE consortium (Angulo et al. 1999). This compilation provides revised nuclear rates and, for the first time, gives the uncertainties associated to these rates which we explored with a parametric code of nucleosynthesis.

1.1 Influence of the NACRE reaction rates on the abundance profiles

In fig.1, we present a comparison between the NACRE rates and earlier ones (Caughlan & Fowler 1988, Champagne et al. 1988, Beer et al. 1991, Iliadis 1990, Gorres et al. 1989) for

*Nuclear Astrophysical Compilation of REaction rates (Angulo et al. 1999)

the main nuclear reactions involving ^{24}Mg and ^{27}Al . Shaded areas represent uncertainties associated to the NACRE reaction rates. The uncertainty domain can be quite large for some rates at the temperatures typical of the Hydrogen Burning Shell inside an RGB star. This may affect the abundance profiles of some elements in stellar interiors.

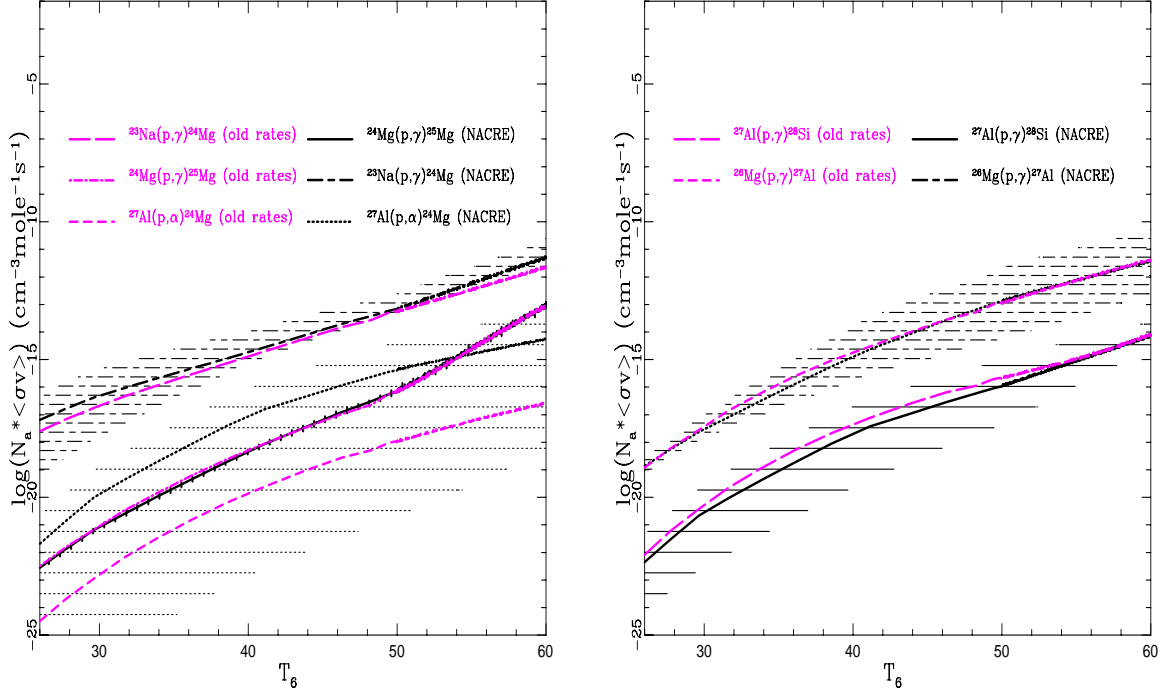


Figure 1: Comparison between the reaction rates recommended by NACRE and the ones from earlier sources (see references in text). Shaded areas represent uncertainty domains given by the NACRE compilation. The temperature domain corresponds to the regions surrounding the HBS between the RGB bump and tip in our model.

Figure 2 presents the abundance profiles for CNO, NeNa and MgAl elements between the bottom of the convective envelope ($\delta M = 1$) and the base of the HBS ($\delta M = 0$), for a star typical of M13 at the tip of the RGB. With the NACRE reaction rates (bold lines), the CNO abundance profiles appear to be very similar to the ones obtained with the reaction rates by Caughlan & Fowler (1988; thin lines). The internal structure of the stellar models thus remains unaffected by using either rates. This enables us to use a parametric code to study the effects of the uncertainties on the reaction rates involved in the NeNa- and MgAl- loops, which appear to be very large in the relevant domains of temperature (fig.1). The profiles of the carbon and oxygen isotopes appear to be fairly well constrained. However quite large uncertainties remain in the profiles (position and abundances) of ^{23}Na and ^{25}Mg which are mainly shifted toward the center or the external layers, and of ^{21}Ne , ^{22}Ne , ^{26}Mg and ^{27}Al . For these isotopes, the maximum and minimum values of their abundances at a given temperature can even change by one order of magnitude.

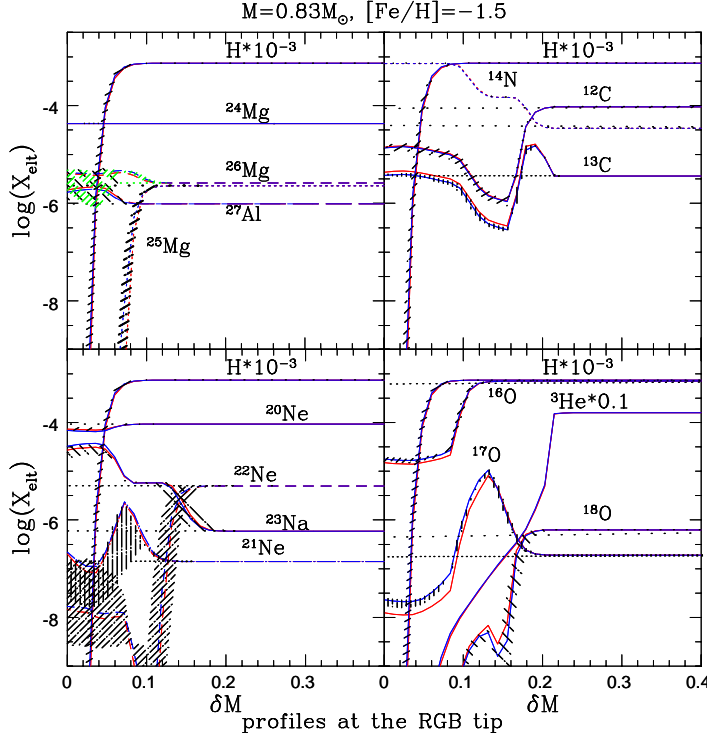


Figure 2: Abundance profiles and uncertainties associated to the NACRE nuclear reaction rates. Bold lines correspond to the NACRE reaction rates and thin ones to earlier sources. δM is defined as : $\delta M = (M_r - M_{core}) / (M_{CE} - M_{core})$

1.2 Impact of the new rates on the evolutionary scenario

Exploring these uncertainty domains, we now present the maximum surface variations of sodium, oxygen, aluminium, etc..., that one can expect to find within the framework of the evolutionary scenario.

In fig.3 and fig.4 we compare the nucleosynthesis predictions (bold lines) with observations. From a nucleosynthesis point of view, enhancements of sodium and depletion of oxygen observed at the surface of many GCRGs can be reproduced assuming that some deep mixing process (which is not taken into account in our model) connects the convective envelope and the regions where the abundance of helium has increased by less than 4%. There, within the more external sodium “plateau”, hydrogen is not depleted yet (see fig.2 and Charbonnel et al. in this volume).

Figure 2 shows that no change in the ^{24}Mg abundance is noticeable with the NACRE rates in such a star as was already the case with previous rates (Denissenkov et al. 1998, Langer et al. 1993, Langer & Hoffman 1993). ^{24}Mg requiring higher temperatures to capture protons ($T \sim 80.10^6$ K), an enhancement of ^{27}Al could only be due to ^{25}Mg abundance decrease and to ^{26}Mg increase, but not to ^{24}Mg destruction. On the other hand, without making any particular assumption on the magnesium isotopic ratios in a M13 typical star ($M = 0.83M_{\odot}$ and $[\text{Fe}/\text{H}] = -1.5$) (Shetrone 1996a and references therein), nucleosynthesis can not account for the observed aluminium enhancements and the Na-O anticorrelation at once as shown in fig.4. We confirm that the aluminium abundance anomalies observed by Shetrone(1996) (^{24}Mg seems to be depleted in Al-rich stars) could be related to primordial contamination. Testing various isotopic ratios for magnesium, it turns out that with $^{24}\text{Mg}/^{25}\text{Mg}/^{26}\text{Mg} \sim 29.4/58.8/11.8$, typical of intermediate mass AGB yields (Forestini & Charbonnel 1997), one could expect a more

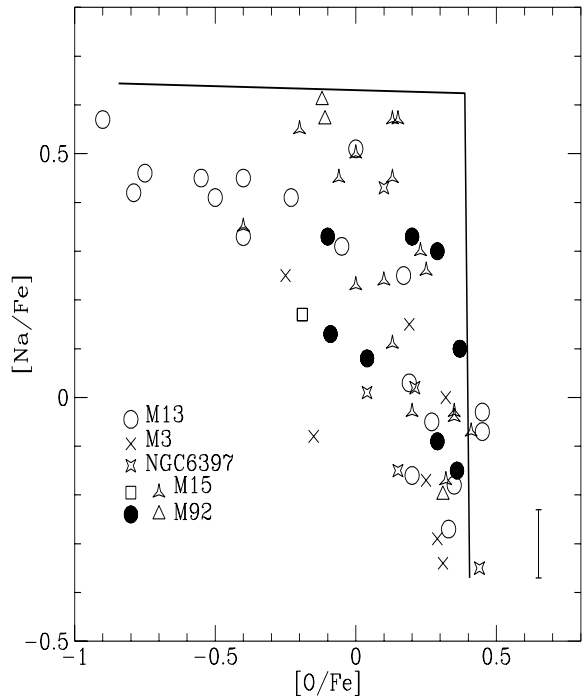


Figure 3: O-Na anticorrelation in different globular clusters (see Charbonnel et al. in this volume for references). The bold line represents the variations obtained for a model typical of a RGB star in M13 ($M = 0.83M_{\odot}$, $[Fe/H] = -1.5$). The typical errorbar for Na abundance is also given.

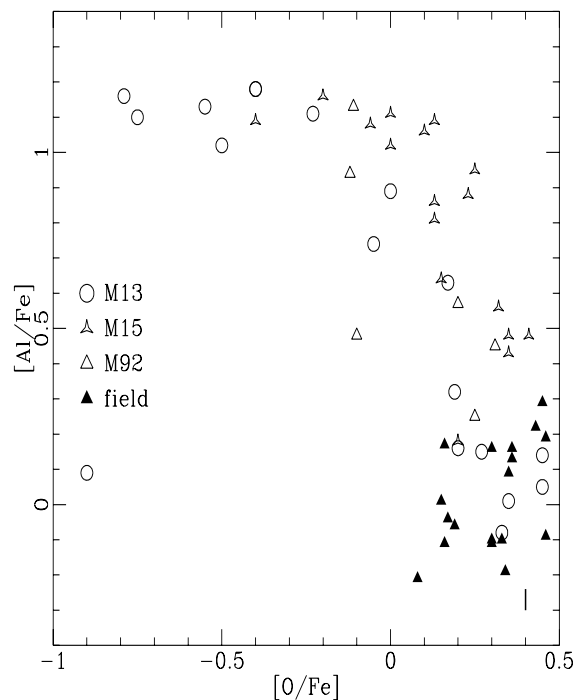


Figure 4: O-Al anticorrelation in different globular clusters and in field stars. The bold line represents Al-variations within the more external sodium “plateau”, which are compatible with the observed O-Na anticorrelation.

important but yet insufficient production of aluminium.

In any case, new determinations of the Mg isotopic ratios in Al-rich RGB stars are necessary to clarify the primordial effects.

2 Nucleosynthesis in an AGB star

The NACRE consortium also provides reaction rates (and their lower and upper limits) for the combustion of helium. We investigate their influence on the evolution of the composition of the helium shell surrounding the C-O core during the AGB phase. The NACRE rates allowed us to show that the reactions responsible for the production of ^{16}O in intermediate mass AGB are well known and constrained. On the other hand, the rate of the reaction $^{22}\text{Ne}(\alpha, n)^{25}\text{Mg}$ is very uncertain (uncertainty domain width : $\sim 10^3 - 10^4$ at $T_8 = 1 - 2$); this prevents from giving good constraints to the production of neutrons in massive AGB stars among other things.

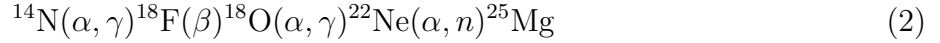
We present here the results of the α -capture nucleosynthesis in the “mean” physical conditions of a thermal pulse inside an AGB, obtained with a simplified parametric code (temperature and density are constant). In particular, we describe in details the variations of the abundances resulting of the two reaction chains involving ^{14}N and ^{18}O , and leading to the production of ^{25}Mg through ^{22}Ne .

During a thermal pulse, ashes from the HBS are melt with helium at average temperature and density of $T_8 = 2.5$ and $\rho = 10^4 \text{ g/cm}^3$. Under these conditions a very rich and unique

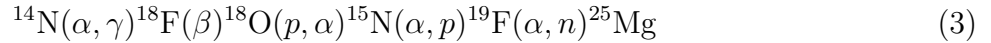
Figure 5: Main nuclear reaction fluxes occurring during a thermal pulse by the light of the NACRE data base. The bolder the arrows, the more important the flux.

nucleosynthesis occurs, as shown in fig.5.

We focus on the three following reaction chains:



and



We can notice that all the reactions involve the capture of an α -particle, except $^{18}\text{O}(p, \alpha)^{15}\text{N}$. In this case, we will show that (n,p) reactions provide the flux of protons necessary to make the (p, α) channel efficient for the destruction of ^{18}O in the third chain.

Proton and neutron sources during a thermal pulse

In fig.5, we present the main nuclear reaction fluxes during the combustion of helium inside the thermal pulse. The 3α reaction produces a large amount of ^{12}C , which, together with ^{13}C (which comes from H-burning ashes), leads mainly to the synthesis of ^{16}O . Indeed, the reactions responsible for the production of ^{20}Ne and ^{24}Mg have sufficiently low rates to keep the abundances of these elements unchanged (reaction chain (1)). The reaction $^{13}\text{C}(\alpha, n)^{16}\text{O}$ is the main source of neutrons in the medium at the beginning of the helium flash, as shown in figure 6. This production of neutrons is directly correlated to the abundance of protons through the reaction $^{14}\text{N}(n, p)^{14}\text{C}$ at this point in the He-burning phase (see fig.6).

Reaction chain (2) is generated by a “ ^{14}N reservoir”, which has been built up during the hydrogen combustion through the CNO cycle. Each element involved in this chain is produced and then destroyed by the capture of an α -particle. Concerning ^{18}O , however, we can notice that the (p, α) channel, even if narrower than the (α, γ) channel, can not be neglected (reaction chain (3)). This is due to the presence of protons in the medium, that we can impute to both $^{14}\text{N}(n, p)^{14}\text{C}$ and $^{26}\text{Al}^g(n, p)^{26}\text{Mg}$ reactions. Indeed, an analysis of the fluxes derived from the NACRE reaction rates shows that these two reactions provide an equivalent amount of protons in so far the abundance of ^{14}N is not negligible. We have already mentioned $^{13}\text{C}(\alpha, n)^{16}\text{O}$ as main supplier of neutrons in the early stages of He-burning, and we can add $^{22}\text{Ne}(\alpha, n)^{25}\text{Mg}$, which takes over at more advanced stages (see fig.6).

References

- Angulo C., Arnould M., Rayet M., et al. (the NACRE collaboration), 1999, Nucl. Phys., A656, 3
- Beer H., Voos F., Winters R.R., 1991 preprint
- Caughlan G. and Fowler W.A., 1988, At. Data Nucl. Data Tables, 40, 207
- Champagne A.E., Cella C.H., Konzes R.T., Loury R.M., Magnus P.V., Smith M.S., Mao Z.Q., 1988, Nucl. Phys. A487
- Denissenkov P.A. and Denissenkova S.N., 1990, Soviet Astron. Lett., 16, 275
- Denissenkov P.A., Da Costa G.S., Norris J.E. and Weiss A., 1998, A&A, 333, 926-941
- Forestini M., and Caughlan G., 1997, A&AS, 123, 241

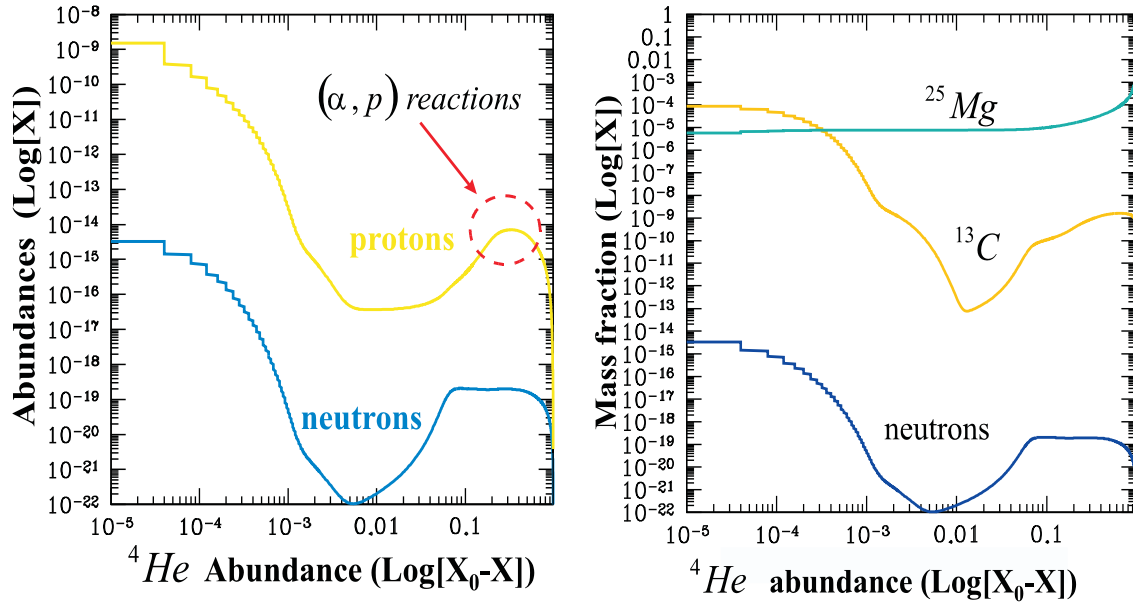


Figure 6: Correlation between the abundances of protons and neutrons (left pannel) and neutrons production (right pannel) as functions of the amount of ${}^4\text{He}$ that has been burnt.

Illiadis C., 1990, Nucl. Phys. A512, 509

Langer G.E., Hoffman R. and Sneden C., 1993, PASP, 105, 301-307

Langer G.E. and Hoffman R., 1995, PASP, 107, 1177-1182

Shetrone M.D., 1996a, AJ 112, 1517

Timmermans R., Becker H.W., Rolfs C., Schroder U., Trautvetter H.P., 1988 Nucl. Phys. A447, 105

